

bs-23926R**[Primary Antibody]****TRPV1 Rabbit pAb****Bioss**
ANTIBODIES

www.bioss.com.cn

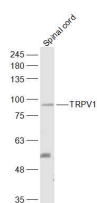
sales@bioss.com.cn

techsupport@bioss.com.cn

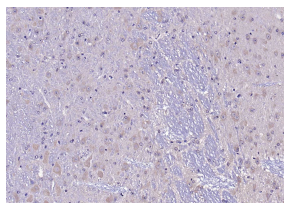
400-901-9800

— DATASHEET —

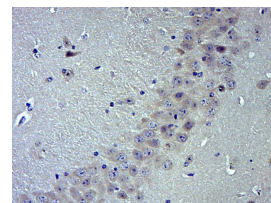
Host: Rabbit Clonality: Polyclonal GeneID: 7442 Target: TRPV1 Immunogen: KLH conjugated synthetic peptide derived from human TRPV1 : 141-240/839. Purification: affinity purified by Protein A Concentration: 1mg/1ml Storage: 0.01M TBS (pH7.4) with 1% BSA, 0.02% Proclin300 and 50% Glycerol. Shipped at 4°C. Store at -20°C for one year. Avoid repeated freeze/thaw cycles. Background: The detection of noxious stimuli (chemical, mechanical, or thermal) occurs predominantly at the peripheral terminals of primary afferent neurons. This information is ultimately transmitted to the central nervous system to evoke a perception of pain which initiates appropriate protective reflexes. The receptor for capsaicin, VR1 (vanilloid receptor 1; TRPV1 is a nonselective cation channel that resembles members of the transient receptor potential (TRP) family of ion channels. The vanilloid receptor 1 protein functions both as a receptor for capsaicin and a transducer of noxious thermal stimuli. VR1 protein is localized to small-diameter sensory neurons within the dorsal root ganglia and nerve terminals in the dorsal horn.	Isotype: IgG SWISS: Q8NER1	Applications: WB (1:500-2000) IHC-P (1:100-500) IHC-F (1:100-500) IF (1:100-500) Reactivity: Mouse (predicted: Human, Rat, Rabbit, Pig, Sheep, Cow, Dog, Horse) Predicted MW.: 92 kDa Subcellular Location: Cell membrane
--	---	---

— VALIDATION IMAGES —

Sample: Spinal cord (Mouse) Lysate at 40 ug
Primary: Anti-TRPV1 (bs-23926R) at 1/1000
Secondary: IRDye800CW Goat Anti-Rabbit IgG at 1/20000 dilution
Predicted band size: 92 kD
Observed band size: 92 kD



Paraformaldehyde-fixed, paraffin embedded (mouse brain); Antigen retrieval by boiling in sodium citrate buffer (pH6.0) for 15min; Block endogenous peroxidase by 3% hydrogen peroxide for 20 minutes; Blocking buffer (normal goat serum) at 37°C for 30min; Antibody incubation with (TRPV1) Polyclonal Antibody, Unconjugated (bs-23926R) at 1:200 overnight at 4°C, followed by operating according to SP Kit(Rabbit) (sp-0023) instructions and DAB staining.



Paraformaldehyde-fixed, paraffin embedded (Mouse brain); Antigen retrieval by boiling in sodium citrate buffer (pH6.0) for 15min; Block endogenous peroxidase by 3% hydrogen peroxide for 20 minutes; Blocking buffer (normal goat serum) at 37°C for 30min; Antibody incubation with (TRPV1) Polyclonal Antibody, Unconjugated (bs-23926R) at 1:400 overnight at 4°C, followed by operating according to SP Kit(Rabbit) (sp-0023) instructions and DAB staining.

— SELECTED CITATIONS —

- **[IF=15.84]** Yuanyuan He. et al. Injectable Affinity and Remote Magnetothermal Effects of Bi-Based Alloy for Long-Term Bone Defect Repair and Analgesia. 2021 May 20 IHC ;Rat. 34014040
- **[IF=6.59]** Yuge Jiang. et al. Eugenol improves high-fat diet/streptomycin-induced type 2 diabetes mellitus (T2DM) mice muscle dysfunction by alleviating inflammation and increasing muscle glucose uptake.. FRONT NUTR. 2022

Important Note: This product as supplied is intended for research use only, not for use in human, therapeutic or diagnostic applications.

Nov;9:1039753-1039753 WB ;Mouse. 36424928

- **[IF=6.208]** Lisha Chen. et al. Silencing P2X7R Alleviates Diabetic Neuropathic Pain Involving TRPV1 via PKCε/P38MAPK/NF-κB Signaling Pathway in Rats. INT J MOL SCI. 2022 Jan;23(22):14141 WB ;Rat. 36430617
- **[IF=5.924]** Hung-Jen Wang. et al. Molecular Effects of Low-Intensity Shock Wave Therapy on L6 Dorsal Root Ganglion/Spinal Cord and Blood Oxygenation Level-Dependent (BOLD) Functional Magnetic Resonance Imaging (fMRI) Changes in Capsaicin-Induced Prostatitis Rat Models. INT J MOL SCI. 2022 Jan;23(9):4716 WB,IF ;Rat. 35563108
- **[IF=4.924]** Haiyang Wang. et al. A Pilot Study of Clinical Evaluation and Formation Mechanism of Irritable Bowel Syndrome-like Symptoms in Inflammatory Bowel Disease Patients in Remission. J Neurogastroenterol. 2021 Oct 30; 27(4): 612–625 WB ;Human. 34642282